Thermal performance of lightweight concrete applications in building envelopes in Lebanon

Emilio Sassine, Elias Kinab, Yassine Cherif, Emmanuel Antczak, Michel Nasrallah

Thermal performance of lightweight concrete applications in building envelopes in Lebanon

Emilio Sassine[1,*]; Elias Kinab[2]; Yassine Cherif[3]; Emmanuel Antczak[3], Michel Nasrallah[4];

[1]Laboratory of Applied Physics (LPA), Lebanese University, Faculty of Sciences, Fanar Campus, Lebanon

[2]Lebanese University, Faculty of Engineering, Roumieh, El Metn, Lebanon

[3]Univ. Artois, ULR 4515, Laboratoire de Génie Civil et géo-Environnement (LGCgE), Béthune, F-62400, France

[4]CC Technique, Memari Street, Hamra, Beirut, Lebanon

Abstract –

Innovative building materials are being used in building envelopes for reducing their heating and cooling needs. This paper aims to assess the thermal impact of using lightweight concrete in Lebanese building constructions by pouring an 8 cm thickness of lightweight concrete on the roof and the slab and replacing traditional hollow concrete block by lightweight concrete blocks.

Thermal properties of two different samples were experimentally determined: the first one (558 kg/m^3) used for the roof and the slab and the second one (1074 kg/m^3) used for the walls. Then numerical simulations were carried out for a Lebanese traditional detached house using the characteristics of these two samples. The thermally improved Light Weight Concrete building (LWC) was compared to a traditional Lebanese house base case (BC) using a dynamic building energy simulation tool in the four different Lebanese climate zones: coastal, mid-mountain, mountain, and inland zones.

The results highlight the effectiveness of integrating LWC to building envelopes by reducing energy consumption and improving thermal comfort in both winter and summer climate conditions and in the different Lebanese climatic zones. The paper demonstrates that the use of LWC in the vertical walls replacing the traditional hollow blocks can reduce the heating needs by up to 9 % and by up to 13 % for cooling needs. On the other hand, adding a LWC roof screed has a very high impact on cooling and heating energy consumption, which can reach up to 74 % in cooling energy savings and up to 24 % in heating energy savings.

Keywords — *Lightweight concrete; thermal properties; building energy simulation; thermal insulation; climatic conditions*

**Corresponding author: Emilio Sassine, emilio.sassine@gmail.com*

Highlights

- Thermal characterization of lightweight concrete samples used for masonry solid blocks and roof screeds
- Determination of the equivalent thermal properties of masonry wall based on the thermal properties of blocks and mortar
- Comparison between the heat transfer in the double wall in the Finite Element Method (FEM) and the Building Simulation Method (BSM).
- Analysis of the building envelope thermal performance and thermal comfort for different scenarios of lightweight concrete integration
- Investigation of the energy saving potential for different scenarios of lightweight concrete integration in the building envelope and in different climate conditions

1 Introduction

Innovative building materials are being used in building envelope to improve its energy consumption, its mechanical properties and to reduce its environmental impact. Lightweight concrete is one of these materials that has many applications in construction.

Effectively, lightweight concrete offers several advantages such as light weight, thermal and sound insulation performance. While normal concrete has a density of around 2,400 kg/m^3, lightweight concrete densities vary between 400 kg/m^3 and 1600 kg/m^3. Many types of concrete fall within this range; some are cellular concretes made with foaming agents and others are made with lightweight aggregates.

Foam concrete, also known as Lightweight Cellular Concrete (LCC) contains a foaming agent that is mixed with mortar. The foam is created by mixing a foaming agent with water and air through a generator.

This material is suitable for a wide range of applications such as panels and blocks production, floor and roof screeds, wall casting, sound barrier walls, void infill, outdoor furniture and many other applications.

Compressive strength of foam concrete ranges from up to 40 MPa down to almost zero for the very low densities. It has many advantages as building material such as thermal and sound insulation, fire rating, and ease of handling. Lightweight Concrete could be used for either on-site casting or concrete block manufacturing.

Many research studies addressed thermal and mechanical modelling of lightweight foam concrete through analytical and numerical models. **Wei et al. (2014)** performed a three-dimensional method for modeling the heat transfer of foamed concretes for densities ranging between 300 and 1700 kg/m^3. **Kumar et al. (2018)** implemented experimental characterization of six batches of foamed concrete with dry densities ranging between 860 and 1245 kg/m^3 and compared them with the clay bricks. The results showed that almost 50 % of the building dead load can be reduced and the thermal resistance can be improved. **Wei et al. (2013)** characterized the microstructures of foamed concrete samples with densities ranging between 300 and 1700 kg/m^3 using 3D by the X-ray computerized tomography to model their 2D microstructures and numerically predict their effective thermal conductivities. **Nguyen et al. (2018)** used the X-ray Computed Tomography (XCT) to characterize the foamed concrete microstructure and failure mechanisms when subjected to compression load. The results showed that foamed concrete is less brittle but has a lower compressive strength compared to normal concrete. **Miled and Limam (2016)** used various analytical models for predicting the thermal conductivity of foam concretes by comparing the results of experimental data with numerical results obtained from 3D Finite Element Method (FEM) simulations.

Moreover, several research studies have recently investigated the improvement of thermal and mechanical properties of foam concrete. **Li et al. (2019)** suggested a novel ultra-light aerogel foam concrete having a very low density (less than 200 kg/m^3) and also a very low thermal conductivity of 0.049 W/(m.K) for potential applications in high energy efficiency buildings. This material was obtained by adding nano-porous aerogels into foam concrete. **Raj et al. (2019)** reported an in-depth review of physical and functional properties and various applications of foamed concrete using various types of foams with various densities varying from 300 to 1800 kg/m^3. The mechanical properties as well as other functional characteristics (thermal and acoustic properties and fire resistance) were discussed. **Li et al. (2020)**

examined the effect of the foaming gas used as well as the cement type on the overall thermal conductivity of the foamed concrete mixture for improving its thermal insulation. **Yoon et al. (2020)** developed a new nano-aerogel material integrated to foam concrete for improving its thermal transfer and moisture resistance. They found that the nano-aerogel embedded in foam concrete decreases by about 30–50 % its thermal conductivity compared to conventional foam concrete with also 75 % lower water absorption. **Hou et al. (2019)** evaluated the effect of nanoparticles, namely nano-SiO_2 (NS) and graphene (G) respectively, on foaming agents for potential improvement of their mechanical properties. A potential improvement of the mechanical properties was identified, however, improvements for other parameters, such as thermal conductivity and water absorption were not obvious when using foaming agents with nanoparticles. **Liu et al. (2018)** found that the foam concrete thermal performance can be greatly improved by using silica aerogel composition. They also performed energy simulations to prove that in both cold and hot climate conditions, the use of Foam Concrete with Silica Aerogel (FC-SA) can greatly reduce energy consumption.

Within this framework, these novel materials need a dynamic analysis at the building scale to study effective building energy performance for real climate considerations. Many building energy simulation tools can be used for predicting the consumed energy for heating and cooling and predicting how buildings perform under different design and engineering scenarios. These tools help in finding and assessing new technical solutions for improving the year-round buildings energy performance.

Various research studies address the lightweight concrete thermal performance at the building scale using building energy simulation models to analyze the building envelope energy performance.

Shen et al. (2018) proposed an energy simulation tool for lightweight buildings and verified the results through EnergyPlus software. **Pak et al. (2018)** studied the thermal performance of a new-design passive house with a double-skin envelope with lightweight concrete in heating and cooling conditions by comparing its energy consumption to a conventional reference house. **Duanmu et al. (2017)** highlighted the effectiveness of foam concrete application in Chinese hot-wall Kang using numerical and experimental approaches. **Roberz et al. (2017)** investigated the energy efficiency and thermal comfort of ultra-lightweight concrete (ULWC) building envelopes compared to more conventional constructions using the analytical EN-ISO13786 calculation methods. The quality of the simulations in EnergyPlus was first ensured through analytical validation, then a case study was performed on commercial and residential buildings in the Netherlands to assess the performance of ULWC.

Furthermore, many research works discussed the heat transfer in masonry walls **(Zhou et al. 2018, Li et al. 2015, Hansen et al. 2018, Knarud and Geving 2017, Odgaard et al. 2018)**, however, the relation between the equivalent thermal properties of the wall and the thermal properties of the blocks and mortar was not explicitly detailed; especially that most of these models rely on 1D equation models which suppose dealing homogeneous uniform building layers.

Narrowing the circle towards a more local setting, this study focuses on light weight concrete LWC applied to Lebanese buildings. The importance of this subject is that Lebanon is a country where nearly 97 % of its energy needs are imported **(Kinab and Elkhoury 2012)**. The industrial sector uses around 25 % of Lebanon's energy consumption, while 30 % is used for the residential, public and commercial sector and the remaining 45% is used in the transportation sector **(World Bank 2009)**.

Lebanese buildings are characterized by their reinforced concrete structures and their vertical walls in single or double wall block masonry. This mode of construction dominates although new technologies have difficulty finding a place in this sector characterized by its high resistance to modifications because of the low-skilled labor force and the low costs of the materials currently used. The thermal performances of these walls remain until now unknown for lack of scientific thermal characterization method at different scales (material, wall, building, etc.).

In this context, this paper highlights the advantages of integrating LWC to building envelopes by comparing the energy consumption and the thermal comfort in both winter and summer climate conditions in different Lebanese climatic zones. The method of determination of the equivalent thermal properties of masonry walls is detailed and a comparison between the heat transfer in the double wall in the Finite Element Method (FEM) and the Building Simulation Method (BSM) is done to validate the adopted method. Then, a base case residential building is compared to thermally improved building scenarios integrating lightweight concrete (LWC) materials in the building envelope, namely the roof and the external walls. Particular attention is given to heat transfer across the walls and the roof for both technologies. Two different lightweight concrete samples were analyzed experimentally and then applied to a detached house case study; the first sample having a lower density is used for the roof screed and the second sample is considered for lightweight masonry blocks manufacturing. The novelty of this work lies in the investigated approach from the material scale to the wall scale up to the building scale, and also in the obtained results showing the effectiveness of light concrete in the Lebanese architectural and climate contexts.

2 Methodology and scope of work

Masonry hollow blocks are the most adopted construction technology in many countries and in particular in the Lebanese context for what they offer of advantages related to their low cost, availability, structural strength, and relatively good thermal performance. These blocks are manufactured in a traditional craft way and are assembled together using mortar joints. The new constructions often present a double wall (10 cm each wall) with air gap space to increase their thermal resistance.

Lightweight concrete materials are nowadays widely used in the building sector and replacing many traditional construction materials for what they offer as advantages in reducing constructions dead loads and making savings in foundations and reinforcement, and improving the thermal properties.

The Aercel® lightweight concrete product is used in the present study, it is a commercial Lebanese product designed for deck roofing and floor applications. It is mainly used to reach effective slopes for proper drainage or for thermal insulation purposes and can also be used for manufacturing lightweight concrete masonry blocks. The concrete mixture is composed of Portland cement, Aercel® lightweight concrete admixture and water, and is produced using the Aercel® foaming machine (Fig. 1).

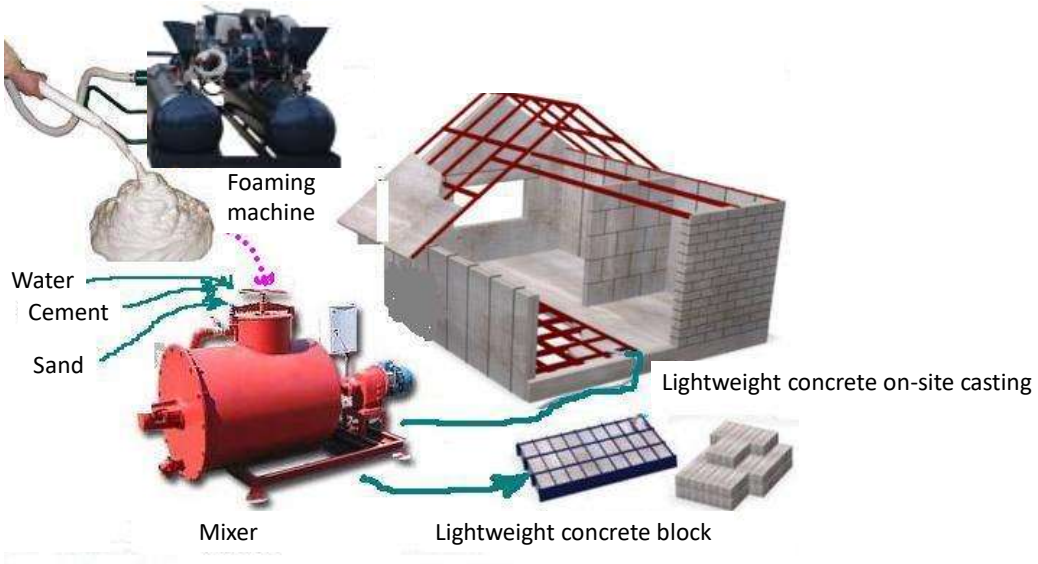

Figure 1- Cellular concrete preparation using Aercel® foaming machine

In this work, a scientific approach is adopted at various scales from the block level, to the masonry wall, to the multilayered wall to end up with a full building simulation in real weather conditions using a Lebanese weather file.

As shown in Fig. 2, in the first section, the lightweight concrete samples, as well as the traditional hollow block and mortar joint, are experimentally tested in order to determine their thermal properties.

Then, in the next section, the equivalent thermal properties of the masonry wall are computed; indeed, the wall layers in building simulation tools are considered homogeneous and their input thermal properties are entered as homogeneous materials while the masonry walls are composed by two different materials and it is therefore necessary to determine their equivalent dynamic thermal properties.

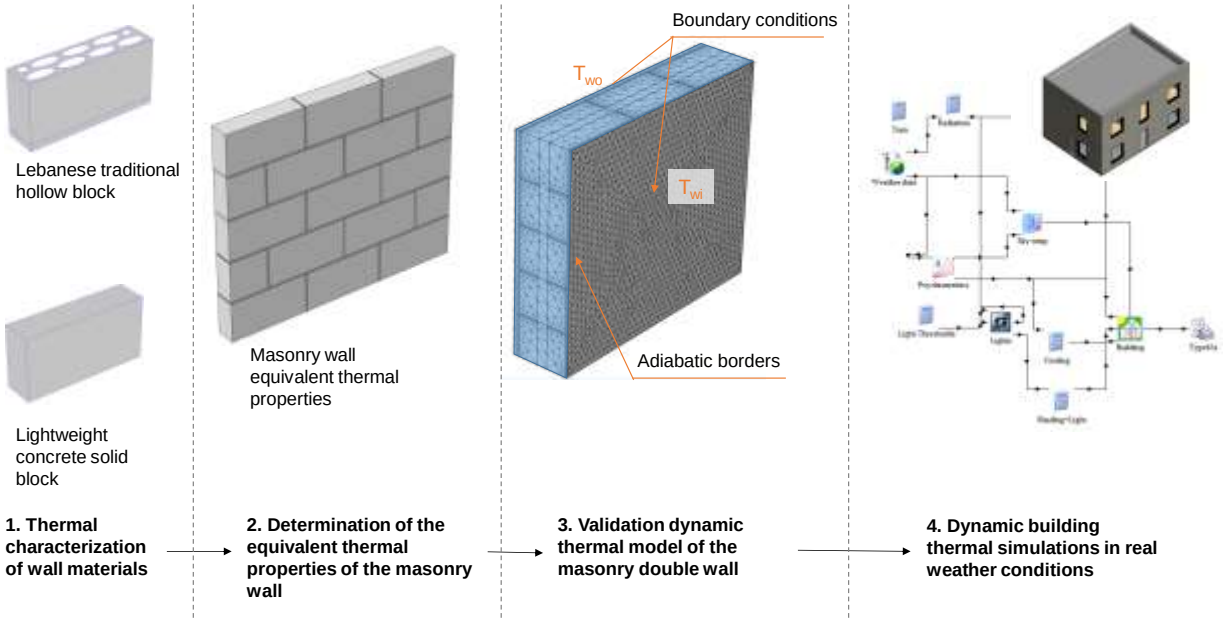

Figure 2- Adopted scientific approach

After determining the equivalent thermal properties of the masonry wall the average heat flux in the Finite Element Model (3D) is compared to the heat flux in the Building Simulation Model (1D) to make sure the two models are equivalent and give similar results. The same inside and outside wall surface computed in the building simulation model using a real weather file (Climate Zone 2 in Lebanon), were applied to the FEM model. The traditional Lebanese wall made of hollow blocks was used for this model validation and the solar radiative gains were removed from the building simulation model in order to make this comparison possible.

In the last section, a residential detached house was used as case study to compare the thermal performance of the base traditional building case to five different scenarios of lightweight concrete integration. The thermal performance of the building envelope was investigated using hourly temperature and heat flux evolution during one representative week in summer conditions and one representative week in winter conditions. Then, the energy consumption of the buildings in the different scenarios and in the different climate zones was computed to assess the potential energy savings that can be reached by integrating lightweight concrete to the building envelope in Lebanese constructions.

3 Experimental characterization of building materials

3.1 Characterization method

3.1.1 Experimental setup

A thermal characterization device of construction materials will determine the thermal properties (thermal resistance and equivalent thermal conductivity) of the concrete hollow blocks.

The Heat flow meter method was considered for the thermal characterization based on the technical standard **DIN EN 12667 (2001)** and using an in-house experimental setup as shown in Fig. 3. An imposed temperature boundary condition was applied on the sample sides and recordings of the temperatures and the heat flux allow the determination its thermal conductivity λ (W/m.K) **(Younsi et al. 2011)**.

In the considered experimental setup, the rectangular-shaped tested specimen is sandwiched between two heat exchanging aluminum plates linked to thermo-regulated baths that ensure the required thermal condition. The thermo-regulated baths allow fast and fine regulation of the injected water temperature with a precision of about ±0.01°C (Julabo Model 34 HE - 1 kW). Thermal grease is applied on the contact surface between the sample and the plate heat exchanger to ensure good thermal exchange between the various elements.

The heat fluxes and the temperatures on both sides of the sample were simultaneously measured by inserting between the exchanging plates and the sample two *T*-type thermocouples with a ±0.1°C precision and two tangential gradient fluxmeters having an active surface of 10 x 10 cm². The fluxmeter type is called ‘‘tangential gradient fluxmeter”, it has a thickness of about 0.5 mm, and a sensitivity of about 80 $\mu V.W^{-1}.m^{-2}$ for an active surface of 10 x 10 cm². The lateral faces of the sample are covered with an

insulation material thereby creating an insulating ring around the sample that minimizes the edge effects and the heat transfer to the external ambient conditions.

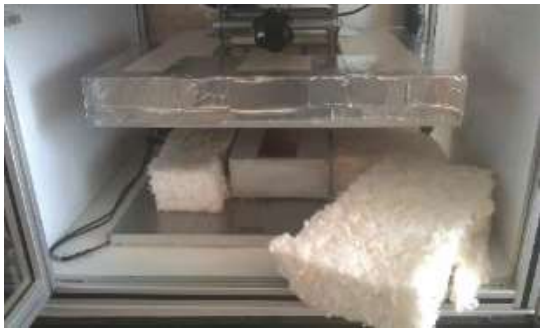

Figure 3- Thermal characterization device for building materials

3.1.2 Calibration and uncertainty

The tangential gradient fluxmeter used in this work (Fig. 4) was used in in several building thermal applications such as the works of **Cherif et al. (2009) and Zalewski et al. (2010)**.

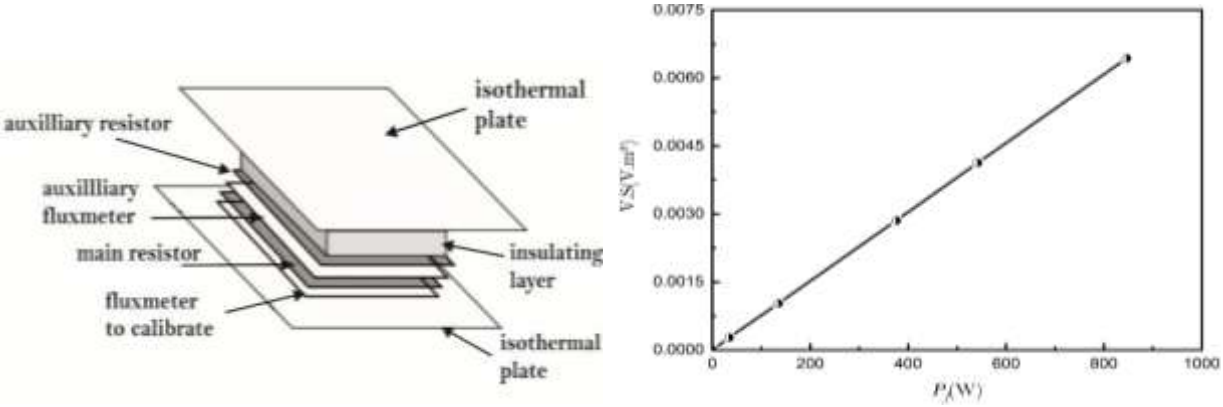

(a) (b)

Figure 4- Schematic drawing of the used heat flux sensors: (a) Heat flux sensor's sketch (b) Calibration apparatus

The calibration of a fluxmeter allows the determination of its sensitivity and its response versus thermal solicitations. Several methods are available in the literature **(Cherif et al. 2009, Zalewski et al. 2010)**. The zero-flux method was used for calibration in this work; it consists in injecting a power into an auxiliary resistance until a zero flux is obtained in the sensor measuring the losses towards the insulator (Fig. 4a). This is possible thanks to a PID (Proportional Integral Derivative) regulator allowing the auxiliary resistor to supply the necessary power.

The operating principle is as follows: the fluxmeter to be calibrated is covered with a heating resistor which dissipates a known amount of heat $P = U^2/R$. An auxiliary fluxmeter is then provided and a second resistor $R_{auxiliary}$ is used to maintain the zero flux measured by the auxiliary sensor. Finally, the whole instrumentation is covered with 5 cm extruded polyurethane in order to limit the external perturbations.

In this device, the energy is supplied to the upper heating resistor in order to cancel the value of the flux measured by the auxiliary fluxmeter. This procedure makes it possible to ensure the passage of the entire heat flux dissipated by the lower resistance in the sensor to be calibrated. The calibration process consists in the measurement of a total thermal power provided by the main heat resistor (Joule effect).

We start with low flux of the order of a few W/m² until about 800 W/m². The results represent an evolution of the "ddp" (potential difference) as a function of the power injected. The sensitivity of the sensor is thus obtained by calculating the slope of the regression line of the cloud of measured points.

The uncertainty for the sensitivity K is given by **Leclercs and Thery 1983**:

$$\Delta K = \left[\left(\frac{\partial K}{\partial V} \Delta V \right)^2 + \left(\frac{\partial K}{\partial S} \Delta S \right)^2 + \left(\frac{\partial K}{\partial v} \Delta v \right)^2 + \left(\frac{\partial K}{\partial I} \Delta I \right)^2 \right]^{1/2} \qquad (1)$$

Where V is the voltage delivered by the sensor, v is the voltage delivered across the main resistor, I is the electric current, and S is the active surface of the fluxmeter.

The fluxmeters are glued with silicon thermal grease and flux lines are parallel and unidirectional both at the inlet and the outlet sides of the sensor**(Lefevbre 1986)**. Fig. 4b shows the calibration curve of the adopted fluxmeters, and confirms the linearity of the response of the sensor over all the tested power range. The voltage response of the fluxmeter is thus proportional to the flux density passing through it.

3.1.3 Characterization method

a.) Thermal conductivity

The method for determining the thermal conductivity consists in subjecting the tested sample to a temperature gradient, and therefore imposing a heat flux transfer from its hot side to its cold side. The heat flux and the temperature on both sides of the sample are measure simultaneously. Fourier's law applied to a unidirectional system in steady state conditions gives:

$$\varphi_1 = \frac{\Delta T}{R} \text{ and } \varphi_2 = \frac{\Delta T}{R} \qquad (2)$$

The thermal conductivity is then given by:

$$\lambda = \frac{e}{R} \qquad (3)$$

b.) Specific heat

Starting from a stable initial steady state, a temperature variation is imposed by changing the set point on one or both sample faces. The average initial temperature of the sample (ΣT_i) will change, as will the fluxes over each side. After the reestablishment of the steady state, the material has found a new stable state, associated with a new average final temperature (ΣT_f).

During the transient phase, the sample stores or releases heat energy Q as its temperature increases or decreases. This energy is related to the heat fluxes difference ($\Delta\varphi$) according to the relation:

$$Q = \int_{t_i}^{t_f} \Delta\varphi.dt \qquad (4)$$

It can also be related to average temperatures $\Sigma T_i/2$ and $\Sigma T_f/2$, where ΣT_i represents the sum of the temperatures on each face at the initial time t_i, and ΣT_f represents the sum of the temperatures on each face at the final time t_f.

$$Q = C\frac{\Sigma T_f - \Sigma T_i}{2} \qquad (5)$$

The heat capacity of the sample is thus given by:

$$C = \frac{2\int_{t_i}^{t_f} \Delta\varphi.dt}{\Sigma T_f - \Sigma T_i} \qquad (6)$$

Knowing the density of the sample and its thickness, the specific heat can be deduced:

$$c_p = \frac{C}{\rho e} \qquad (7)$$

3.2 Experimental results

Two samples were prepared and analyzed in the Laboratory of Civil Engineering and geo-Environment, Artois University. The first sample of lower density is used as roof screed on any flat roof for insulation and roof sloping for rainwater drainage. The second one that has a slightly higher density (medium density) can be used for manufacturing lightweight concrete blocks used to replace hollow concrete blocks in masonry walls.

The tested lightweight concrete samples, shown in Fig. 5, are both 10 cm x 10 cm x 10 cm, the low density lightweight concrete has a density of 558 kg/m^3, while the medium density lightweight concrete has a density of 1074 kg/m^3.

(a) (b)

Figure 5- Low density (a) and medium density (b) lightweight concrete samples

Fig. 6 and Fig. 7 show the temperatures and heat flux measurements for the low density and medium density LWC samples respectively with a time step of one minute.

The low density lightweight concrete sample cold side is set to a temperature T_1 of 15 °C, while its hot side has three steps of temperature T_2: 25, 35 and 45 °C.

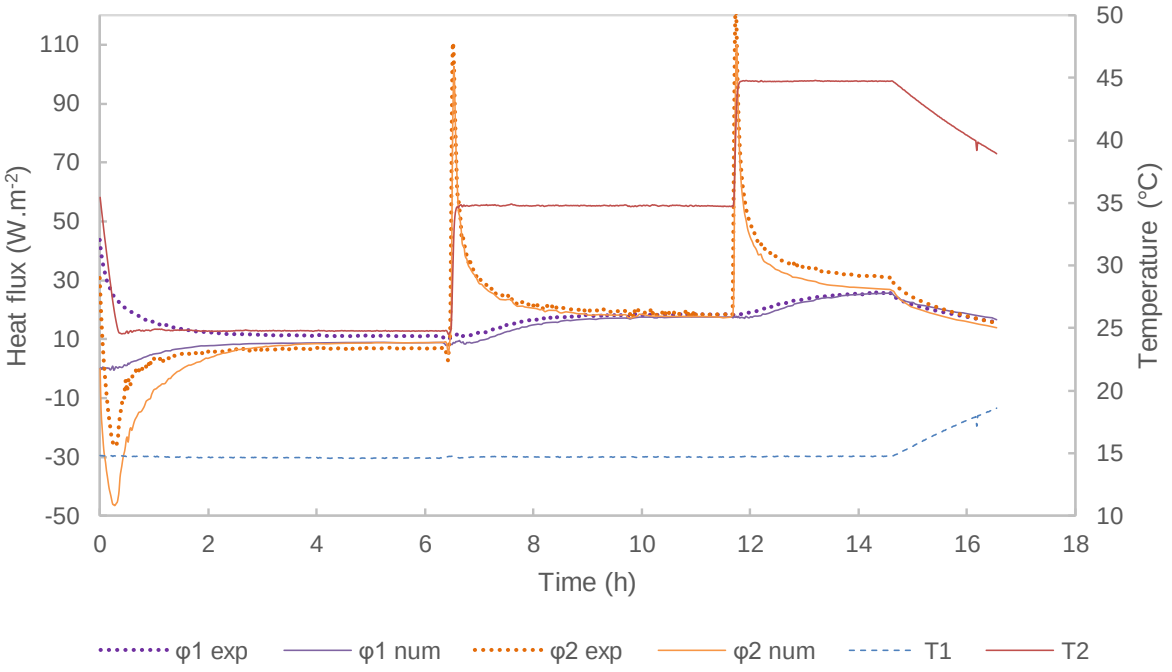

Figure 6- Experimental results for low density lightweight concrete sample

For the case of the medium density lightweight concrete sample, the hot sample side it is initially set to a temperature T_2 of 25 °C for 3.5 hours then to a temperature of 35 °C for the next 2.5 hours while the cold side temperature is maintained at 15 °C.

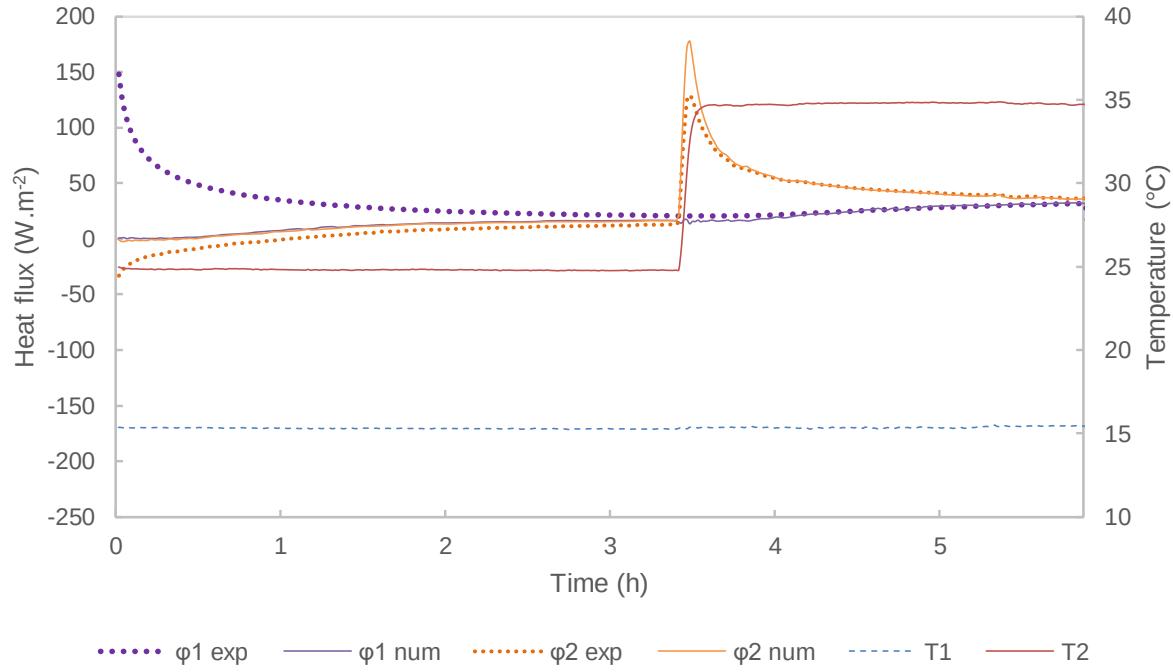

Figure 7- Experimental results for medium density lightweight concrete sample

Then, based on these measurements and Eq. 2 to Eq. 7, the thermal properties of the LWC are computed and reported in Table 1.

Table 1- Thermal properties of the lightweight concrete samples

	Thermal conductivity ($Wm^{-1}.K^{-1}$)	Density (kg/m^3)	Specific heat ($J.kg^{-1}.K^{-1}$)
Low density lightweight concrete sample	0.088	558	447
Medium density lightweight concrete sample	0.178	1074	474

A comparison is performed between the experimental measurements of the heat fluxes evolution at the boundaries of the block and the numerical simulations of the heat transfer in these samples using the Finite Element Method (FEM) in COMSOL Multiphysics® software considering the thermal properties of the lightweight concrete samples found (Table 1) as input for the numerical simulation.

The simulated and measured heat flux are very similar for the two samples as show in Fig. 6 and Fig. 7, except for the first part (between 0h and 2h) where the heat flux depends mainly on the material history (initial conditions) and the heat stored in the material before starting the tests.

Similarly, the thermal properties of the concrete hollow block and mortar joint were determined experimentally and are reported in Table 2.

Table 2- Experimental thermophysical properties of concrete hollow block and mortar joints

Material	Density ($kg.m^{-3}$)	Thermal conductivity ($W.m^{-1}.K^{-1}$)	Specific heat ($J.kg.K^{-1}$)
Cement mortar	1863	1.41	1077
Hollow block	1477	0.63	836

4 Validation of the wall heat transfer numerical model

4.1 Determination of the thermal properties of the equivalent masonry walls

Masonry walls are made of two main components: the blocks and the mortar used to glue these blocks and give structural rigidity to the walls. It is therefore essential to determine the equivalent thermal properties of these walls allowing to have an equivalent homogeneous material with equivalent thermal properties making it possible to introduce it into buildings thermal simulation software.

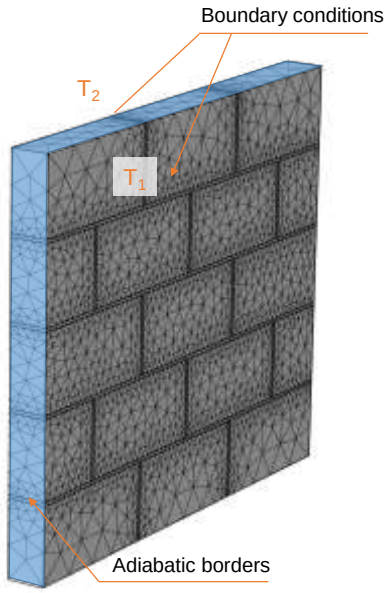

Figure 8- Boundary conditions for the numerical calculation of the equivalent thermal properties of masonry walls

To do so, the wall was modelled and simulated using the FEM in COMSOL Multiphysics® with two different theoretical Dirichlet boundary conditions (imposed temperatures) for defining its equivalent thermal capacity $(\rho c_p)_{eq}$ and its equivalent thermal conductivity λ_{eq} (Fig. 8):

- Stationary study: $T_1 = 40$ °C, $T_2 = 20$ °C
- Time dependent simulation: initial temperature: 20°C, boundary conditions: $T_1 = T_2 = 40$ °C.

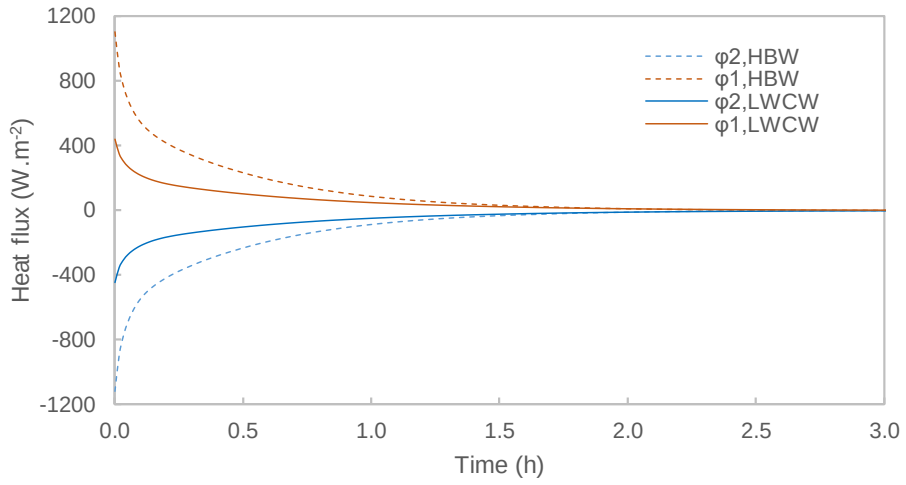

Figure 9- Heat flux evolutions for the HBW and the LWCW for the calculation of the equivalent thermal capacity

The equivalent thermal conductivity λ_{eq} is thus calculated from Eq. 2 and Eq. 3 based on the numerical computed average heat flux on the wall in the stationary simulation study.

The equivalent thermal capacity $(\rho c_p)_{eq}$ can also be calculated using Eq. 6 and Eq. 7 based on the numerical computed heat flux represented in Fig. 9 on the wall in the time dependent simulation study for the hollow block masonry wall (HBW) and for the lightweight concrete masonry wall (LWCW).

Therefore, the equivalent thermal properties for the hollow block masonry wall (HBW) and for the lightweight concrete masonry wall (LWCW), using the same mortar joint type, are reported in Table 3.

Table 3- Experimental thermophysical properties of hollow block masonry wall (HBW) and for the lightweight concrete masonry wall (LWCW)

Wall type	λ_{eq}, $W.m^{-1}.K^{-1}$	$(\rho c_p)_{eq}$ $(J.m^{-3}.K^{-1})$
HBW	0.675	1216000
LWCW	0.249	566400

It is important to note that the equivalent thermal properties λ_{eq} and $(\rho c_p)_{eq}$ are just theoretical values that are used as input parameters in the BSM software and are different than the thermophysical properties of the LWC solid blocks or the hollow blocks.

4.2 Validation of the dynamic behavior of the double wall

The validation of the heat transfer model by comparing the Finite Element Method (FEM) and the Building Simulation Method (BSM) is essential to make sure that the 3D multilayered masonry wall is well represented in the 1D BSM Software. The traditional Lebanese double wall was used for the model validation. The wall composition is represented in Fig. 10. The equivalent thermal properties of the HBW were used in the TRNSYS® BSM software with a total simulation duration of 800 hours (slightly more than one month). The thermal properties of the different layers as well as the thermal properties of the layers of all the building components are reported in Table 5.

The North wall was considered for the validation model and solar gains were removed by assuming a Sky factor equal to zero. Internal gains as well as solar gains were also neglected for the model validation. The purpose is to simplify the boundary conditions on the simulated wall and reduce them to the inside and outside wall temperatures T_{wi} and T_{wo}. The wall surface temperatures as well as the internal and external heat fluxes computed in the BSM were then used for the model validation using the FEM.

The validation was done by imposing the same temperatures T_{wi} and T_{wo} on the 3D wall model and comparing the internal and external heat fluxes φ_i and φ_o in the FEM and in the BSM.

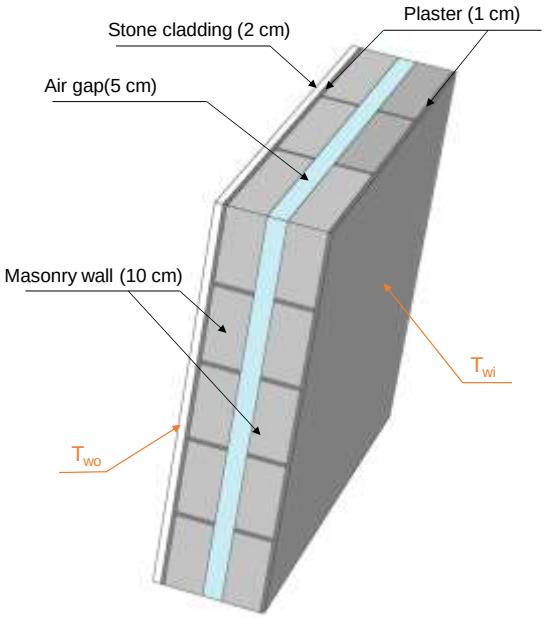

Figure 10- Simulated wall for model validation

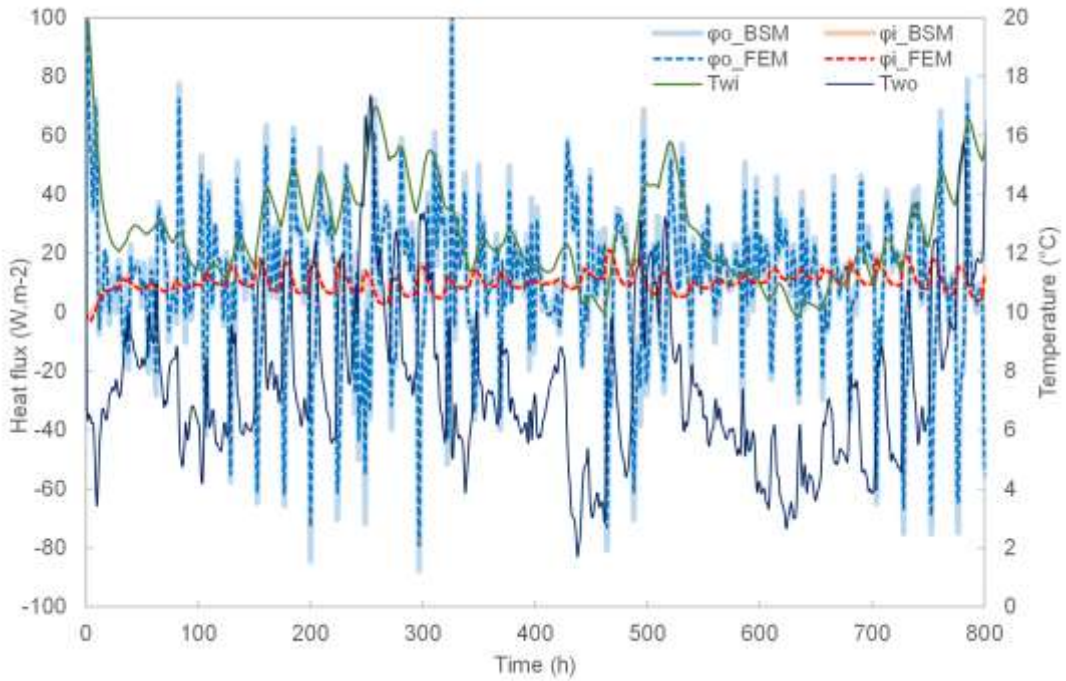

Figure 11- Comparison of the internal and external heat fluxes φ_i and φ_o between the FEM and the BSM

Fig. 11 shows that the FEM and the BSM provide very similar results for both internal and external heat fluxes φ_i and φ_o having the same wall surface temperatures T_{wi} and T_{wo}.

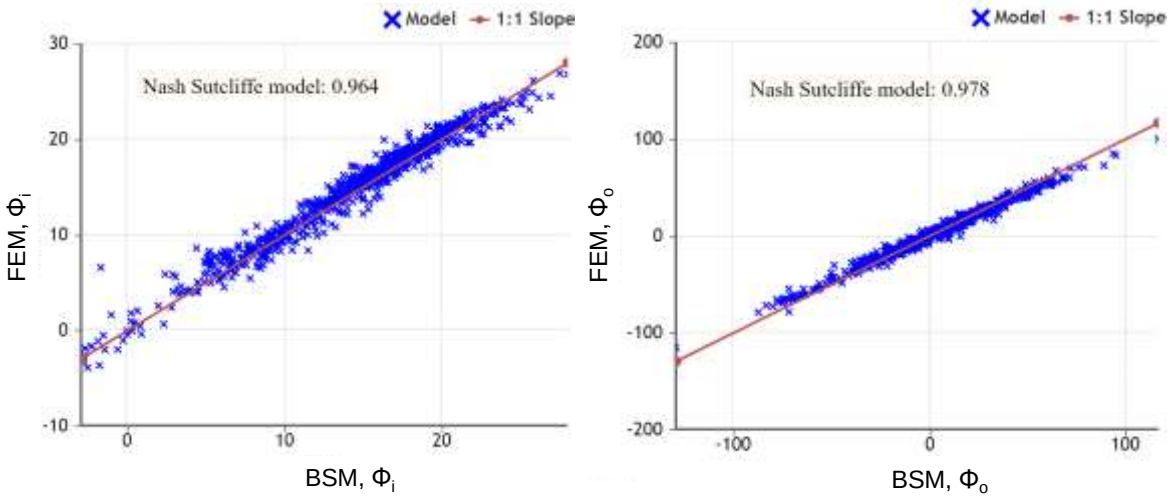

(a) (b)

Figure 12- Nash Sutcliffe model for φi (a) and φo (b)

In order to define how well the measured and simulated heat fluxes are identical, the Nash-Sutcliffe efficiency coefficient (NSE) **(AgriMetSoft 2019)** was used for φ_i and φ_o as shown in Fig. 12. It indicates how well the plot of measured versus simulated model data fits the 1:1 line. A value of *NSE*=1, corresponds to a perfect match of the model to the measurements; *NSE*=0, indicates that the model predictions are as accurate as the mean of the measurements data; and a negative value of *NSE*, indicates that the observed mean is a better predictor than the model.

The results indicate a perfect match between the BSM and the FEM with NSE values close to 1 for both φ_i and φ_o.

5 Building case study

5.1 Geographical and climate context

Although Lebanon is a small Mediterranean country covering an area of only 10 452 square kilometers, it has however four different climate zones adopted by the Thermal Standards for Buildings in Lebanon **(ALMEE 2010)** (Fig. 13): The Coastal Zone (Zone 1), the Western Mid-Mountain Zone (Zone 2), the Inland Plateau (Zone 3), and the High Mountain Zone (Zone 4) **(Lebanese Ministry of Public Works and Transport General Directorate of Urban Planning 2005)**. In order to assess possible effects of climate on thermal performance and design strategies, a representative location for each zone was selected.

Four different locations representing the four main Lebanese climate zones were selected for the simulation: Abdeh (Zone 1), Kleyaat (Zone 2), Tal Amara (Zone 3), and Bcharre (Zone 4); their respective locations are also shown in Fig. 13.

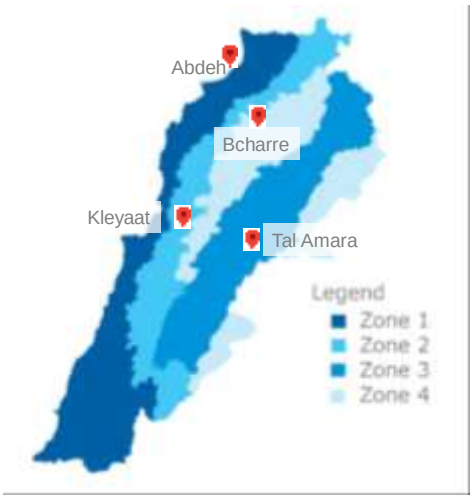

Figure 13- Climate zones and chosen simulation locations

The average daily temperature per month as well as the average daily horizontal solar radiation per month for the four chosen locations are shown in Fig. 14.

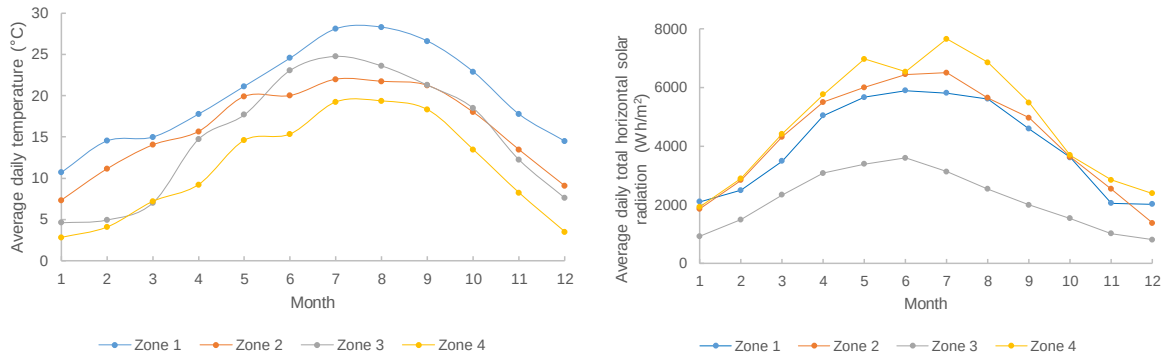

(a) (b)

Figure 14- Average daily temperature per month (a) and average daily horizontal solar insolation per month (b)

5.2 Building description

5.2.1 Building geometry and building envelope

The studied building is a (10.5 m x 7.15 m) typical residential Lebanese two story detached house with a total area of 150 square meters. The building is shown in Fig. 15 and will be studied for the four Lebanese climate zones.

The building envelope composition for the Base Case building used in this study is described in Table 4, and the thermophysical properties of the different envelope layers are listed in Table 5.

The roof is composed of a Reinforced Concrete slab (28 cm) with interior cement plaster (2 cm) and painting. An equivalent one-layer RC slab having a thickness of 30 cm was thus considered for simplification purposes since the cement mortar and the RC slab have comparable thermal properties and the mortar thickness is negligible compared to the concrete in the roof.

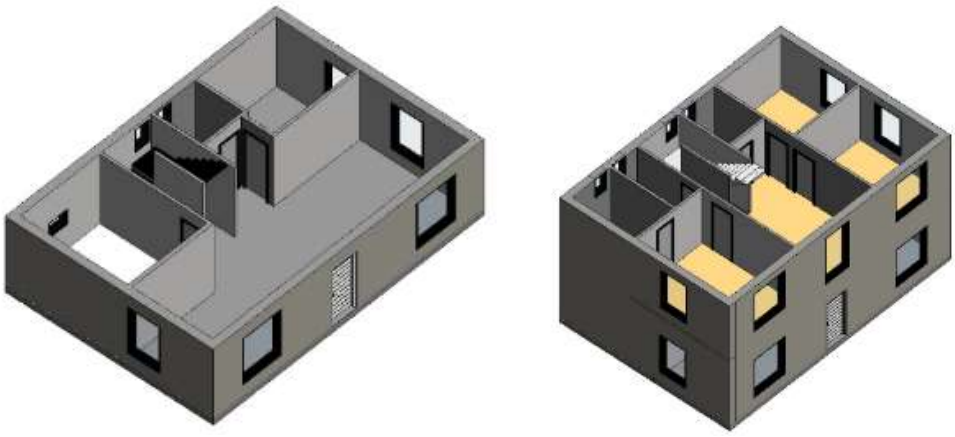

(a) (b)

Figure 15- Ground floor (a) and first floor (b) 3D views of the studied building

Table 4- Envelope composition (from outside to inside) of the Base Case simulated building

Component	Layers (Ext-Int)	Thickness (cm)
Wall	Stone cladding	2
	Cement plaster	1
	Hollow block	10
	Air gap	5
	Hollow block	10
	Cement plaster	1
Roof	RC slab	27
Ground floor	RC slab	30
	Mortar	2
	Stone tiling	2
Glazing	Double glazing	-

Table 5- Thermophysical properties of the materials accounted in the simulated building

Materials	Conductivity k (W/m.K)	Density d (kg/m^3)	Specific heat c (J/kg.K)
Concrete	2.1	2400	800
HBW	0.675	1216	1000
LWCW	0.249	556	1000
LWC 600	0.09	558	447
Plaster and Mortar	1.41	1863	1077
Stone cladding and tiling	3.00	2500	1000

Simulation scenarios:

In addition to the Base Case, five different simulation scenarios were considered. The scenarios differ in how LWC materials are integrated to the building envelope:

In scenario 1 (S1), the base case double wall made of two 10 cm hollow block walls (HBW) separated by an air gap of 5 cm is replaced by a single wall made of 15 cm LWC solid blocks.

In scenario 2 (S2), the inside 10 cm layer of HBW in the base case is replaced by a 10 cm layer of LWC solid blocks while the outside layer of HBW is kept the same.

In scenario 3 (S3), the outside 10 cm layer of HBW in the base case is replaced by a 10 cm layer of LWC solid blocks while the inside layer of HBW is kept the same.

In scenario 4 (S4), the inside and outside 10 cm layers of HBW in the base case are replaced by a 10 cm layers of LWC solid blocks.

Scenario 5 (S5) has the same wall configuration as S4 but is also using an 8 cm of low density LWC screed for the roof from outside.

The U-values of the different building components in the different scenarios are summarized in Table 6.

Table 6- U-values ($W.m^{-2}.K^{-1}$) of the different building components in the different scenarios

	BC	S1	S2	S3	S4	S5
Wall	1.523	1.264	1.101	1.101	0.862	0.862
Roof	3.349	3.349	3.349	3.349	3.349	0.834
Ground floor	2.996	2.996	2.996	2.996	2.996	2.996
Glazing	2.269	2.269	2.269	2.269	2.269	2.269

5.2.2 Main assumptions and simulation scenarios

TRNSYS Software was used for dynamic building energy simulation. Surface temperatures and heat fluxes for the different building envelope components were chosen as outputs in addition to the total sensible heat and the indoor air temperature.

The chosen base temperatures are 20 °C for heating and 24 °C for cooling. The case study building was considered to be reasonably tight with an air change rate of about one air change per hour (n=1 volume/hour).

The Type 56 component was used to model the thermal behavior of the building using a pre-processing program, the TRNBUILD program for creating the so-called building file.

The presence pattern has an important effect on energy consumption and this was recalled in many research works **(Dong et al. 2018, Cuerda et al. 2019, Chen et al. 2018, Muroni et al. 2019)**. In the present study, the objective is more concentrated on the building envelope parameters, the occupancy was therefore simplified and fixed to four people with a day/night schedule where people are present every day from 3 pm till 8 am. The internal gains due to people were selected according to the ISO 7730 norm with people considered at rest and the gains due to artificial lighting were considered to be 5 W/m^2. No shading systems were considered and thermal losses by transmission through thermal bridges were also neglected in this study.

The calculation of the different thermal bridges was performed using the FEM in COMSOL multiphysics® and referring to the **French thermal regulation RT 2012**.

The linear heat loss coefficient can thus be determined using the following equation:

$$\psi = \frac{\varphi_T}{\Delta T} - \sum_{i=1}^{N} U_i L_i \quad \mathrm{W/(m.K)} \qquad (8)$$

Where,

Ψ is the linear heat loss coefficient of the thermal bridge expressed in W/(m.K),

ϕ_T is the total flow per meter of length through the 2D model, expressed in W / m,

ΔT is the temperature difference between the two environments hot and cold, expressed in K,

U_i is the surface heat loss coefficient of component i, expressed in W/(m^2.K),

L_i is the interior length to which the U_i value applies in the 2D geometric model, expressed in m,

N is the number of 1D components.

Table 7- Envelope composition (from outside to inside) of the Base Case simulated building

Configuration	Detail	φ_t (W.m^{-2})	U_i x L_i (W/m.K)	ΔT (K)	Ψ (W/m.K)	Linear heat loss (W/K)
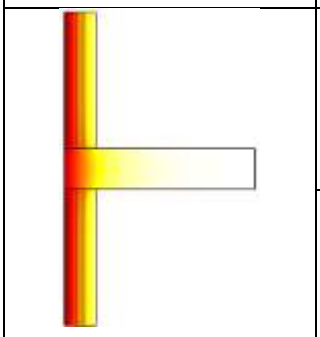	HBW/Concrete intermediate slab	90.81	3.24	20	1.30	45.93
	LWCW/Concrete intermediate slab	59.71	1.78	20	1.21	42.59
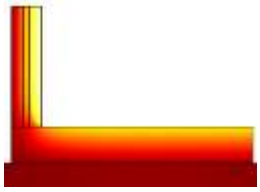	HBW/Concrete lower slab	156.36	7.57	20	0.25	8.77
	LWCW/Concrete lower slab	140.38	6.84	20	0.18	6.34
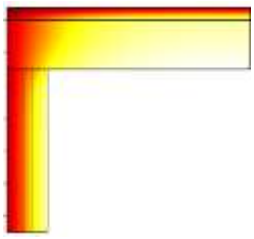	HBW/Concrete roof	117.31	5.02	20	0.85	29.83
	LWCW/Concrete roof	101.38	4.29	21	0.54	18.97
	HBW/LWC roof	69.25	2.59	20	0.88	30.94
	LWCW/LWC roof	53.65	1.86	21	0.70	24.67

By comparing the difference between the linear heat losses in the different configurations (different scenarios) shown in Table 7, one can conclude that this difference is not considerable (with a maximum about 11 W/K) and thus the thermal bridges in the different scenarios are comparable. The thermal bridges in winter conditions can thus be considered as equilibrated by the overestimation of solar gains since solar shadings were not accounted in the studied building case.

In the first part, we will analyze the hourly thermal performance of the building envelope and the thermal comfort during one cold winter week from January 10th till January 16th and one warm summer week from July 10th to July 16th by using the weather conditions of Zone 1 as external boundary conditions. The evolution of the heat transfers through the building envelope as well as the indoor thermal comfort will be investigated for the base case and the LWC in scenarios 1 to 5.

Then, in the second part, the yearly cooling and heating energy needs for the different scenarios and in the different Lebanese climate zones will be analyzed in order to assess the thermal performance of lightweight concrete applications in building envelopes in Lebanon.

6 Results and discussion

6.1 Building envelope thermal analysis

For a better understanding of the thermal behavior of the building envelope in winter and summer conditions, a comparison between the base case (BC) and the five LWC scenarios (S1-S5) was performed during one representative week in winter (January 10th till January 17th) and one representative week in summer (July 10th till July16th) using climate Zone 1 for comparison because it possesses a relatively cold winter and a relatively hot summer so the comparison can be done in these two extreme seasons..

6.1.1 Analysis of the vertical walls

The hollow block double wall of the base case was compared to the four configurations presented in scenarios 1-4. The observation of the heat flux through building envelope allow to understand how the energy flow is taking place inside and outside the building in winter and summer conditions and compare the thermal inertia and thermal resistance of the different configurations.

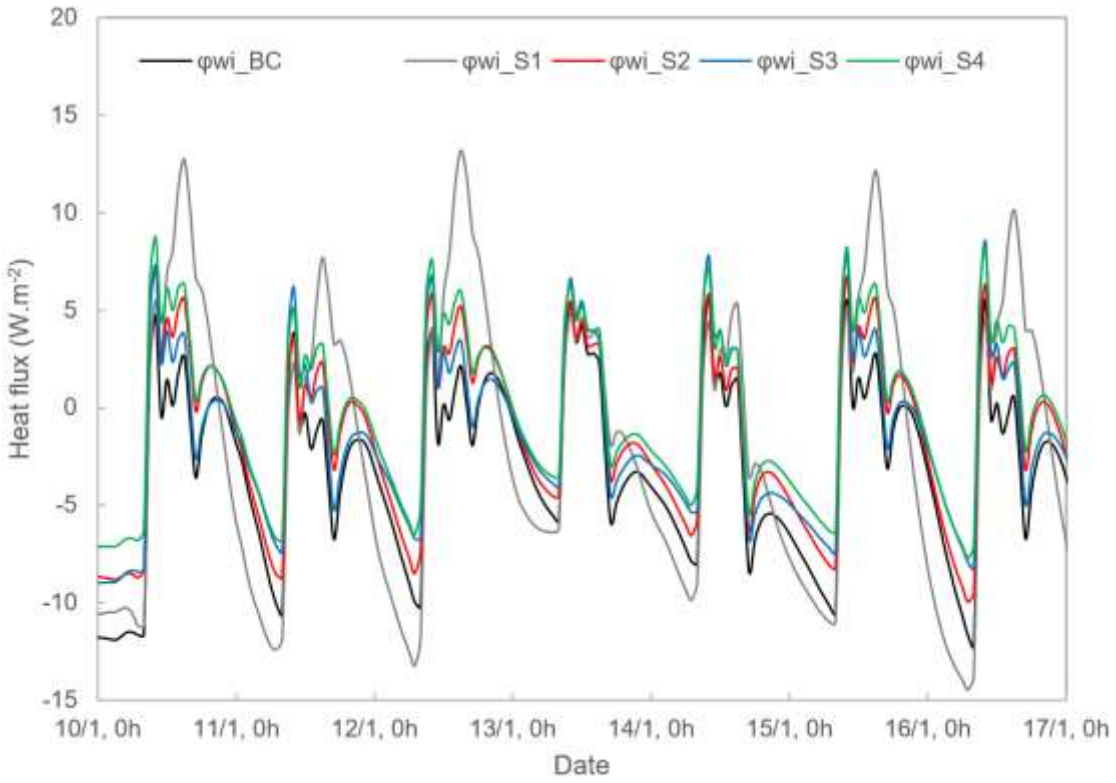

Figure 16- Energy heat flow through the walls in Winter conditions

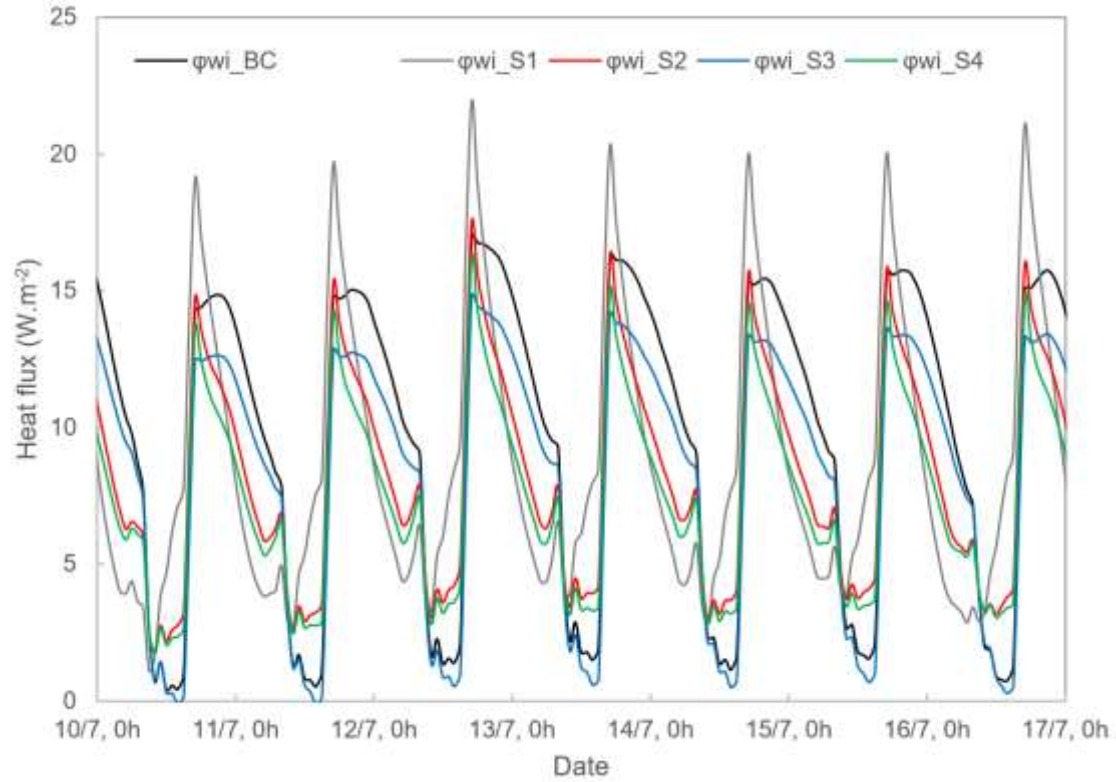

Figure 17- Energy heat flow through the walls in Summer conditions

The single lightweight wall in scenario S1 presents higher peaks of heat flux than the remaining scenarios in both winter (Fig.16) and summer (Fig.17) conditions due to its lower heat capacity compared to the other configurations.

Moreover, S3 is slightly better than S2 due to its better heat capacity, in fact the traditional hollow block is heavier and has a higher thermal capacity, this is why having an outside LWCW layer and inside HBW (S3) is better than having outside HBW layer and inside LWCW (S2). This effect is more clearly noticed in summer conditions were the peaks of heat flux in S3 are less pronounced than S2.

S4 is slightly better than the other scenarios in winter conditions but has a similar performance in summer conditions.

The indoor wall temperature is also an important thermal comfort indicator. Indeed, uninsulated walls emit cold radiation, which make the occupants uncomfortable even if the air in the room is sufficiently heated. These cold walls are therefore a source of heat loss, condensation and discomfort. The more the temperature is homogeneous in the different areas of the habitat, the more the sensation of comfort is high. The analysis of the indoor surface temperature for the walls in the different scenarios in winter (Fig. 18) and summer (Fig. 19) conditions also confirms the conclusions drawn from observations of the heat fluxes evolution.

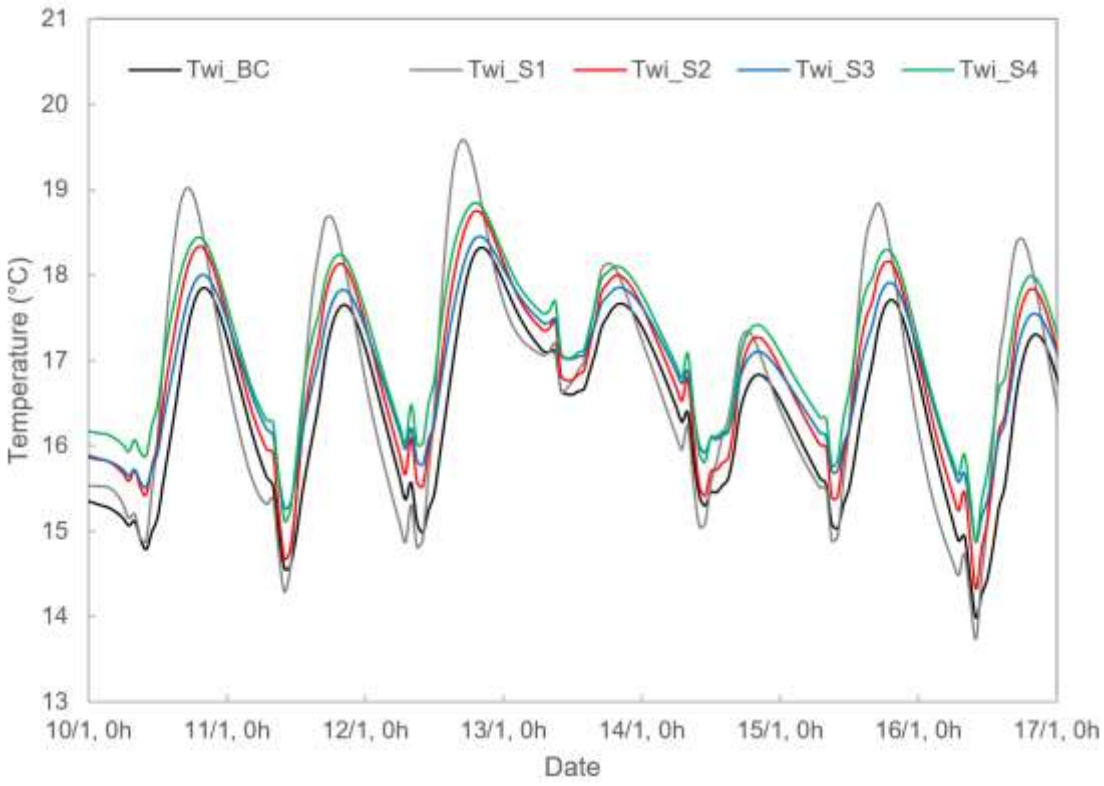

Figure 18- Indoor wall temperature in Winter conditions

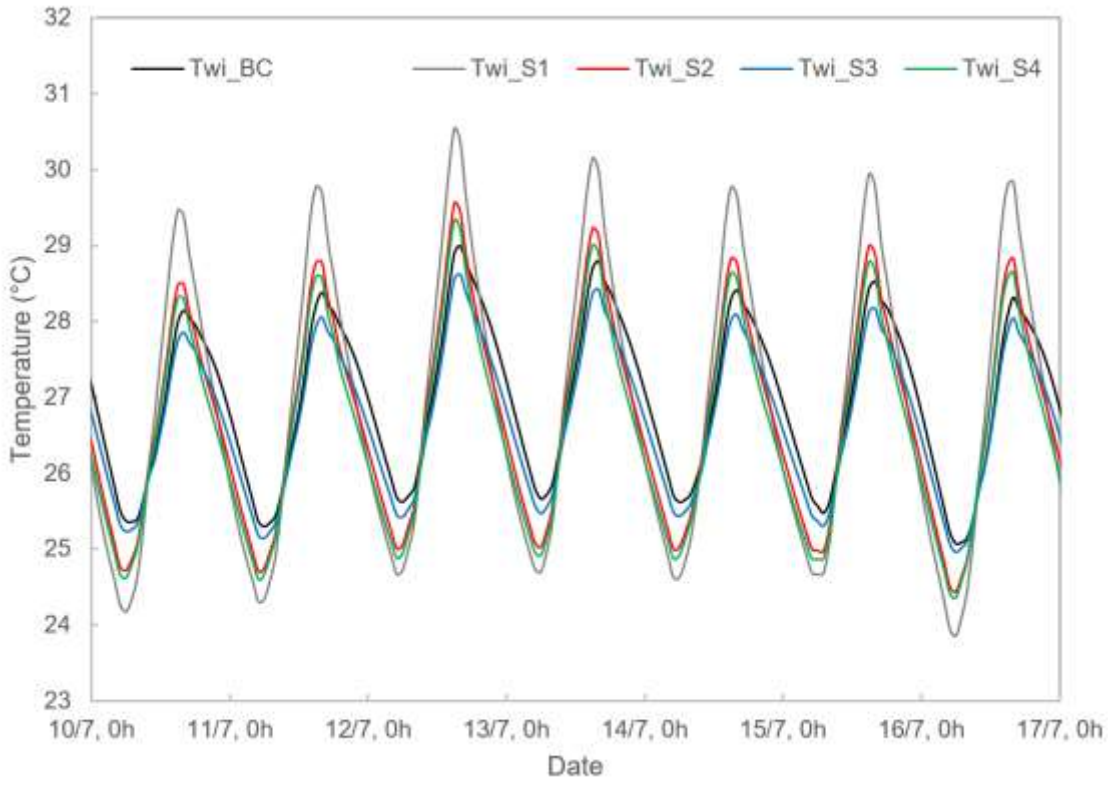

Figure 19- Indoor wall temperature in Summer conditions

In brief, the scenario S1 also presents higher peaks of temperature than the remaining scenarios in both winter (Fig.18) and summer (Fig.19) conditions due to its lower heat capacity compared to the other configurations. As well, S3 is slightly better than S2, S4 and BC during the day time in Summer conditions while the BC represents the lower temperature fluctuations due to the fact that traditional hollow block is heavier and has a higher thermal capacity than LWC block.

6.1.2 Analysis of the roof

The effect of adding an 8 cm LWC layer screed to the roof is assessed by comparing the indoor surface temperature and heat flux between the BC and S5.

During winter (Fig. 20), the roof in the base case is subjected to a very pronounced heat flux variation (solar gains) while the roof in S5 performs much better with a flatter curve and lower values of the heat flux. Same observations are noticed for the temperature variations where it varies between 12 °C and 17 °C in the BC while it varies only between 16 °C and 18 °C for S5 in winter conditions.

Similarly, during summer (Fig. 21), the high peaks of heat flux as well as the temperature peaks reaching 32 °C in the BC may cause overheating of the rooms and lead to thermal discomfort. These observations disappear in S5 where the heat flux and temperature profiles seem to be more damped which will improve the thermal comfort in summer conditions.

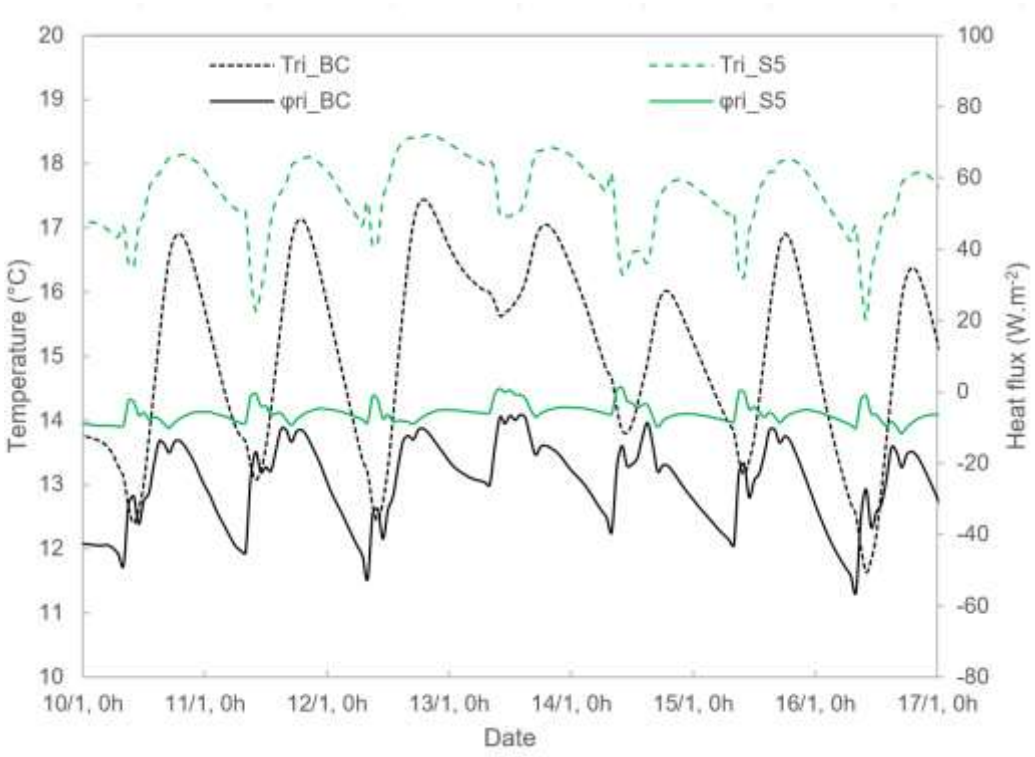

Figure 20- Heat flow and temperature of the roof from inside in winter conditions

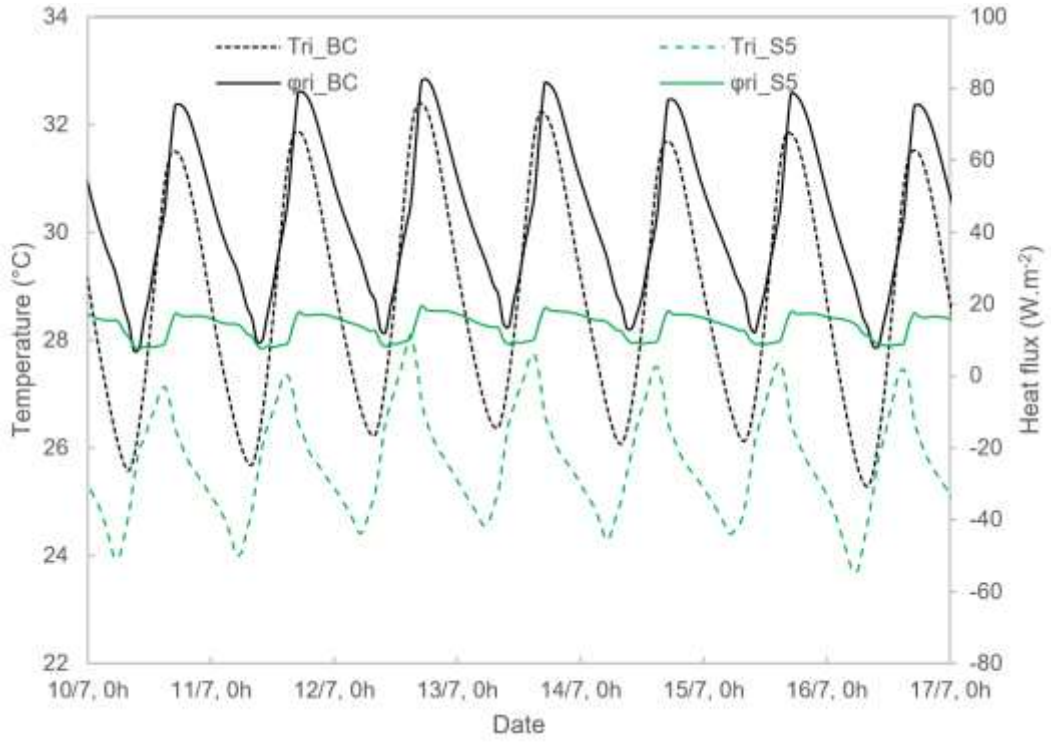

Figure 21- Heat flow and temperature of the roof from inside in summer conditions

6.2 Analysis of the building energy needs

Fig. 22 shows that heating and cooling energy needs vary widely between the different climate zones. Indeed, the heating needs for the base case vary from around 58 kWh/m^2/year in Zone 1 (Coastal Zone) to around 100 kWh/m^2/year in Zone 2 (Mid-mountain Zone), and about 153 in kWh/m^2/year Zone 3 (Inland Zone), reaching a maximum of about 196 kWh/m^2/year in Zone 4 (High Mountain Zone). Cooling loads on the other hand are considerable in Zone 1 with around 33 kWh/m^2/year but less important for zones 2, 3, and 4 with less than 20 kWh/m^2/year.

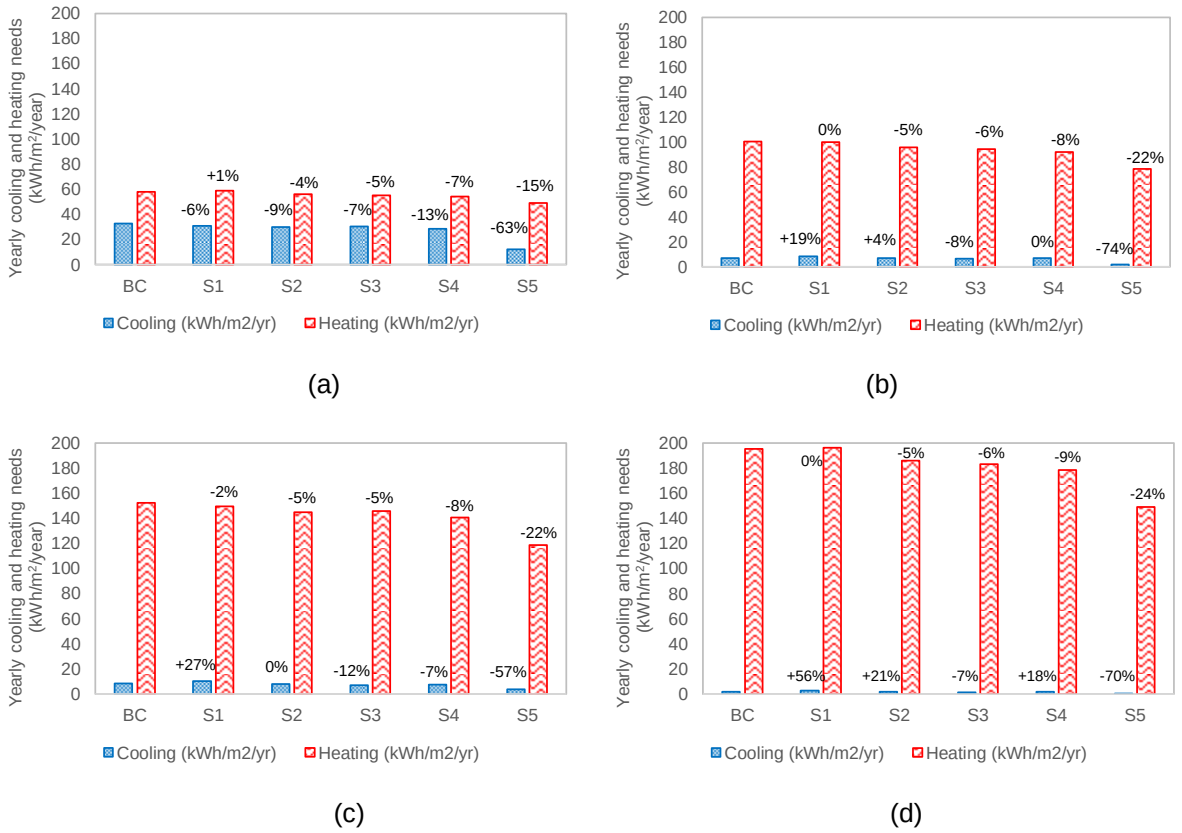

Figure 22- Cooling and heating needs for the different scenario cases, in zone 1 (a), zone 2 (b), zone 3 (c), and zone 4 (d)

In Zone 1 (Fig. 22a) where both heating and cooling exist, replacing the traditional double wall by a single lightweight concrete wall has almost similar impact on heating needs but cooling needs can be reduced by about 6 %. This solution is thus interesting not only from a thermal point of view, but also from a practical and economic view since it allows reducing the space loss by reducing the wall thickness and the material and labor cost due to building a single wall instead of a double wall. The effect of adding the roof screed on reducing the heating needs and especially cooling needs are clearly shown by comparing S4 and S5.

The same observations can be done for heating needs in Zones 2, 3, and 4, while the cooling needs in these zones are very low.

6.3 Analysis of the building energy consumption

For a better understanding of the energy consumption related to the base case and the considered improvement scenarios, five different heating systems and two different cooling systems commonly used in the Lebanese context were analyzed. For heating, two central systems were considered, a central heating system based on a diesel boiler and radiators and a central air conditioning system. In addition, three other decentralized systems were considered to be used in the different building spaces to cover the building heating needs; these systems include a gas heaters using gas tanks, electric heaters, and split air conditioning units. Split and central AC systems were compared for cooling.

Heating and cooling energy consumptions were first analyzed, then the energy bills were compared in order to have the same reference for comparison.

The energy efficiency, energy cost, and calorific values for the different investigated systems are described in table 8. The energy cost values are based on the Lebanese market rates.

Table 8- Characteristics of the selected heating and cooling systems

	Diesel boiler	**Gas heater**	**Electric heater**	**Split air conditioning**	**Central air conditioning**
Calorific value	10 kWh/liter	13.6 kWh/kg	-	-	-
Energy efficiency (-) / Coefficient of performance (-)	0.9	1	1	3.2	2.8
Energy cost	0.525 $/liter	1.01 $/kg	0.2 $/kWh	0.2 $/kWh	0.2 $/kWh

The yearly heating and cooling energy bills for the different heating systems, for the different scenario cases in the different climate zones are compared in Fig. 23 and Fig. 24. The results clearly disadvantage the use of electric heaters in winter with respect to the remaining heating systems. Indeed, these systems are widely spread across the country for their relatively low cost however they lack of safety and they lead to relatively high energy bills compared to the other options. Gas heaters are also widely used in Lebanon and also present a relatively low investment cost, however, they offer a much better yearly energy cost compared to electric heaters. The best heating option is the central diesel boiler; however, it requires a high investment cost. Split air conditioning systems offer a good compromise between the yearly energy cost and the investment cost and have the advantage to be used also for cooling. The use of a central air conditioning system offers a lower investment cost compared to using multiple split air conditioning systems; however, it leads to a slightly lower efficiency due to energy losses in the air distribution ducting network. The energy consumption for cooling is the highest in zone 1 while it is very negligible in zone 4 where cooling can be neglected.

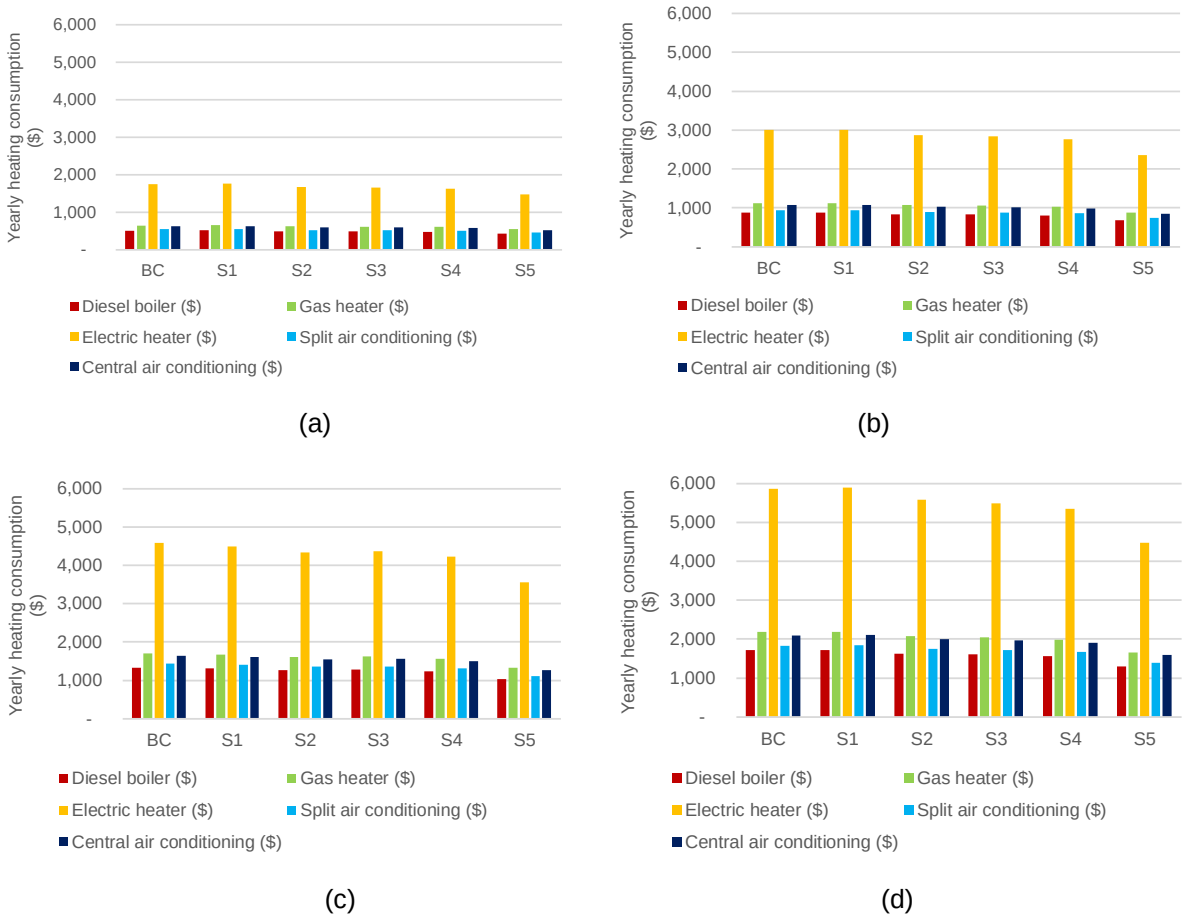

Figure 23- Heating energy bills for different heating systems and in the different scenario cases, in zone 1 (a), zone 2 (b), zone 3 (c), and zone 4 (d)

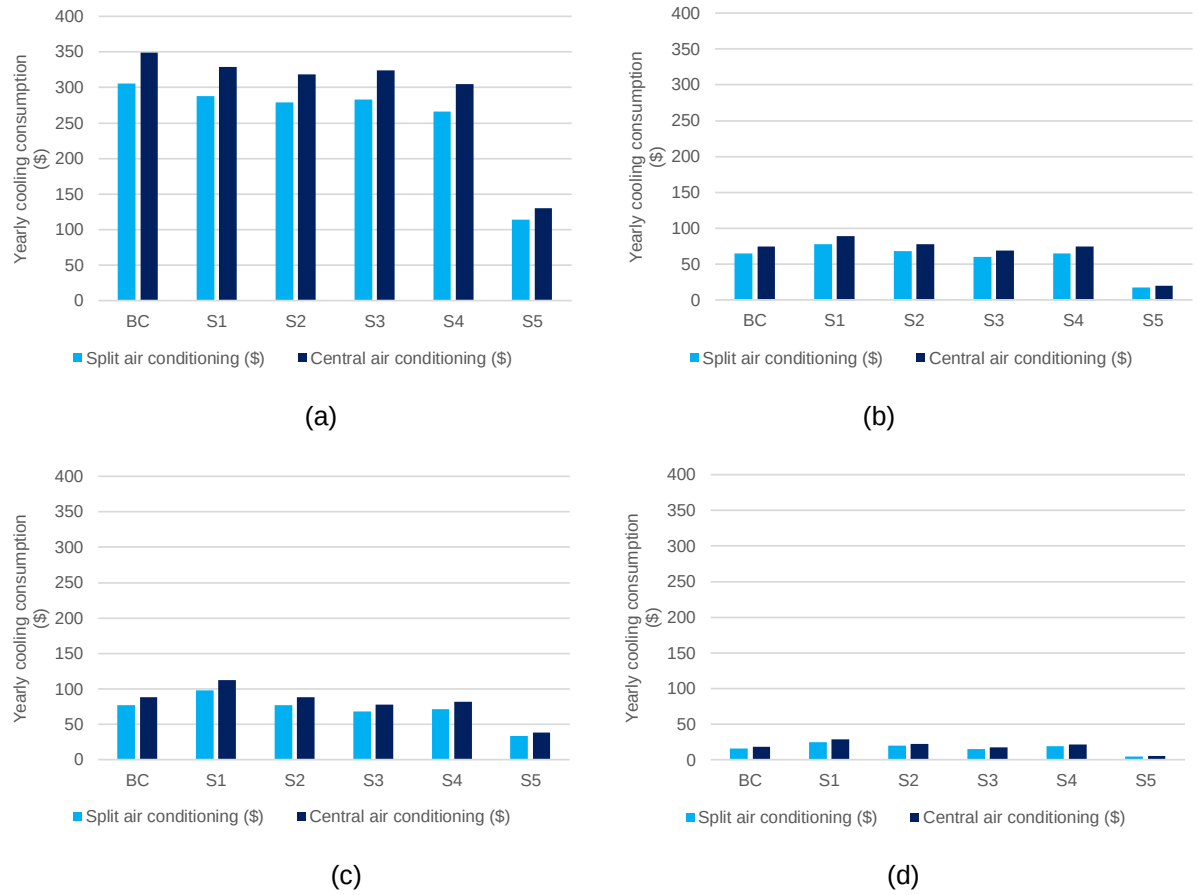

Figure 24- Cooling energy bills for different heating systems and in the different scenario cases, in zone 1 (a), zone 2 (b), zone 3 (c), and zone 4 (d)

7 Conclusions

This paper presented a comprehensive case study for assessing the effectiveness of light concrete in the Lebanese architectural and climate contexts by assessing the thermal performance on different levels from the material scale, to the wall scale, up to the building scale.

Two lightweight concrete samples used for LWC solid blocks and roof screed respectively were experimentally tested to determine their thermal properties. Then, the equivalent thermal properties of the HBW and the LWCW were determined followed by a comparison between the average heat flux in the FEM and the BSM in order to validate the methodology and the model.

A residential detached house was used as case study to compare the thermal performance of the BC with five different scenarios of lightweight concrete integration. The results highlight the effect of LWC in the Lebanese context by showing that their use in the vertical walls replacing the traditional hollow blocks can reduce the heating needs by 4 to 9 % in the four different climatic zones and by 7 to 13 % for cooling needs in Zone 1. On the other hand, adding a LWC roof screed has a very high impact on cooling and heating energy consumption, which can reach up to 63 % in cooling energy savings for Zone 1 and up to 24 % in heating energy savings for Zone 4. A comparison between different heating and cooling systems shows the importance of the system selection on the yearly energy bills. The use of electric heaters is not

recommended even though it is widely spread across the country. Air conditioning systems can be a suitable choice for a moderate investment and a moderate energy bills especially in Zone 1 while the central boiler heating system is recommended in zone 4 offering the lowest yearly heating bill.

This study offers important results for investigating quantitatively and qualitatively the effect of LWC on space heating and cooling in the Lebanese context and in the different Lebanese climatic zones. A financial analysis needs to be performed in the upcoming studies helping to draw more conclusions about the optimal scenarios at both environmental and economic levels.

Conflict of Interests

The authors declare no conflict of interests regarding the publication of this paper.

References

[1] ALMEE (2010). Thermal Standards for Buildings in Lebanon TSBL.

[2] Ministry of Public Works and Transport General Directorate of Urban Planning (2005). Climatic Zoning for Buildings in Lebanon.

[3] AgriMetSoft (2019). Online Calculators. Available on: https://agrimetsoft.com/calculators/Nash%20Sutcliffe%20model%20Efficiency%20coefficient

[4] Chen Y, Hong T, Luo X (2018). An agent-based stochastic Occupancy Simulator. Building Simulation, 11: 37–49.

[5] Cherif Y, Joulin A, Zalewski L, Lassue S (2009). Superficial heat transfer by forced convection and radiation in a horizontal channel. International Journal of Thermal Sciences, 48: 1696–1706.

[6] Cuerda E, Guerra-Santin O, Sendra JJ, González JN (2019). Comparing the impact of presence patterns on energy demand in residential buildings using measured data and simulation models, Building Simulation, 12: 985–998.

[7] Dong B, Yan D, Li Z, Jin Y, Feng X et al. (2018). Modeling occupancy and behavior for better building design and operation—A critical review. Building Simulation, 11: 899–921.

[8] Duanmu L, Yuan P, Wang Z, Xu C (2017). Heat transfer model of hot-wall Kang based on the non-uniform Kang surface temperature in Chinese rural residences. Building Simulation, 10: 145–163.

[9] French thermal regulation: “Réglementation Thermique 2012” RT2012, available online: http://www.rt-batiment.fr/presentation-a12.html

[10] Hansen TK, Bjarlov SP, Peuhkuri RH, et al., (2018). Long term in situ measurements of hygrothermal conditions at critical points in four cases of internally insulated historic solid masonry walls. Energy and Buildings, 172: 235-248.

[11] Hou L, Li J, Lu Z, Niu Y, Jiang J, Li T, (2019). Effect of nanoparticles on foaming agent and the foamed concrete”. Construction and Building Materials 227: 116698.

[12] Kinab E and Elkhoury M (2012). Renewable energy use in Lebanon: Barriers and solutions. Renewable and Sustainable Energy Reviews, 16: 4422-4431.

[13] Knarud JI, Geving S (2017). Comparative study of hygrothermal simulations of a masonry wall. Energy Procedia, 132 : 771-776.

[14] Kumar NV, Arunkumar C, Senthil SS (2018). Experimental Study on Mechanical and Thermal Behavior of Foamed Concrete. Materials Today: Proceedings, 5: 8753–8760.

[15] Leclercs D, Thery P (1983). Apparatus for simultaneous temperature and heat flow measurements under transient conditions. Review of Scientific Instruments 54, 374.

[16] Lefebvre J (1986). Mesure des débits et des vitesses des fluides (Ed) Masson.

[17] Li J, Cao W, Chen G (2015). The heat transfer coefficient of new construction – Brick masonry with fly ash blocks. Energy, 86: 240-246.

[18] Li P, Wu H, Liu Y, Yang J, et al. (2019). Preparation and optimization of ultra-light and thermal insulative aerogel foam concrete. Construction and Building Materials, 205: 529–542.

[19] Li T, Huang F, Zhu J, Tang J, Liu J (2020). Effect of foaming gas and cement type on the thermal conductivity of foamed concrete. Construction and Building Materials, 231: 117197.

[20] Liu S, Zhu K, Cui S, Shen X, Tan G (2018). A novel building material with low thermal conductivity: Rapid synthesis of foam concrete reinforced silica aerogel and energy performance simulation. Energy and Buildings, 177: 385-393.

[21] Miled K, Limam O (2016). Effective thermal conductivity of foam concretes: Homogenization schemes vs experimental data and FEM simulations. Mechanics Research Communications, 76: 96-100.

[22] Muroni A, Gaetani I, Hoes P, Hensen JL (2019). Occupant behavior in identical residential buildings: A case study for occupancy profiles extraction and application to building performance simulation. Building Simulation, 12: 1047–1061.

[23] Nguyen T, Ghazlan A, Kashani A, Bordas S, et al. (2018). 3D meso-scale modelling of foamed concrete based on X-ray Computed Tomography. Construction and Building Materials, 188: 583–598.

[24] Odgaard T, Bjarløv SP, Rode C (2018). Interior insulation—Characterisation of the historic, solid masonry building segment and analysis of the heat saving potential by 1d, 2d, and 3d simulation. Energy and Buildings, 162: 1-11.

[25] Pak R, Ocak Z, Sorgüven E (2018). Developing a passive house with a double-skin envelope based on energy and airflow performance. Building Simulation, 11: 373–388.

[26] Raj A, Sathyan D, Mini KM (2019). Physical and functional characteristics of foam concrete: A review. Construction and Building Materials, 221: 787–799.

[27] Roberz F, Loonen RC, P.Hoes P, Hensen JL (2017). Ultra-lightweight concrete: Energy and comfort performance evaluation in relation to buildings with low and high thermal mass. Energy and Buildings, 138: 432-442.

[28] Shen P, Brahamb W, Yi Y (2018). Development of a lightweight building simulation tool using simplified zone thermal coupling for fast parametric study. Applied Energy 223: 188–214.

[29] Technical Standard DIN EN 12667 (2001). Thermal performance of building materials and products - Determination of thermal resistance by means of guarded hot plate and heat flow meter methods - Products of high and medium thermal resistance.

[30] Wei S, Yiqiang C, Yunsheng Z, Jones MR (2013). Characterization and simulation of microstructure and thermal properties of foamed concrete. Construction and Building Materials, 47: 1278–1291.

[31] Wei S, Yunsheng Z, Jones MR, (2014). Three-dimensional numerical modeling and simulation of the thermal properties of foamed concrete. Construction and Building Materials, 50: 421–431.

[32] World Bank (2009). "Energy efficiency study in Lebanon", Econoler International, REF :5515.

[33] Yoon H, Lim T, Jeong S, Yang K (2020). Thermal transfer and moisture resistances of nano-aerogel-embedded foam concrete. Construction and Building Materials, 236: 117575.

[34] Younsi Z, Zalewski L, Lassue S, Rousse DR, Joulin A (2011). A novel technique for experimental thermophysical characterization of phase-change materials. Int. J. Thermophys, 32: 674–692.

[35] Zalewski L, Lassue S, Roussel D, Boukhalfa K (2010). Experimental and numerical characterization of thermal bridges in prefabricated building walls. Energy Conversion and Management, 51: 2869–2877.

[36] Zhou X, Carmeliet J, Derome D (2018). Influence of envelope properties on interior insulation solutions for masonry walls. Building and Environment, 135: 246-256.